Research Article | Vol. 31, No. 10 / 8 May 2023 / Optics Express 16508
Optics EXPRESS

Generalized multi-cavity laser self-mixing interferometry based on scattering theory

AJIT JHA,[1,*] LINGA REDDY CENKERAMADDI,[2] AND SANTIAGO ROYO[3]

[1]Department of Engineering Sciences, University of Agder, 4879 Grimstad, Norway
[2]Department of Information and Communication Engineering, University of Agder, 4879 Grimstad, Norway
[3]Center for Sensors, Instruments and System Development, UPC-BarcelonaTech, 08222 Terrassa, Spain
[*]ajit.jha@uia.no

Abstract: We present a generalized mathematical model and algorithm for the multi-cavity self-mixing phenomenon based on scattering theory. Scattering theory, which is extensively used for travelling wave is exploited to demonstrate that the self-mixing interference from multiple external cavities can be modelled in terms of *individual* cavity parameters *recursively*. The detailed investigation shows that the equivalent reflection coefficient of coupled multiple cavities is a function of both attenuation coefficient and the phase constant, hence propagation constant. The added benefit with *recursively* model is that it is computationally very efficient to model large number of parameters. Finally, with the aid of simulation and mathematical modelling, we demonstrate how the individual cavity parameters such as cavity length, attenuation coefficient, and refractive index of *individual* cavities can be tuned to get a self-mixing signal with optimal visibility. The proposed model intends to leverage system description for biomedical applications when probing multiple diffusive media with distinct characteristics, but could be equally extended to any setup in general.

1. Introduction

In the case of self-mixing interferometry (SMI) (also know as optical feedback interferometry (OFI), the electromagnetic radiation emitting from the laser is forced to reflect back to its own cavity after reflection from an external (vibrating) target. The change in round trip time from the coupled external cavity changes the emission phase and frequency. This frequency modulated reflected radiation beat with the emanating field inside the laser's cavity to give rise to self-mixing interference causing modulation of output optical power (OOP) and forming interference fringes. These fringes are detected photodiode to get self-mixing signal (SMS) [1–3].

Authors in [1,2,4] explained SMI phenomenon using coupling between electric field and carrier density in the compound cavity, where first cavity is the laser's cavity and second formed by laser's facet and the external target. The general SMI field equation is obtained by adding the external feedback field to the standard lasing field. In this model, the equivalent reflection coefficient of the compound cavity is a function of reflection coefficients of the cavity boundaries (i.e., laser facet and the remote external target). Though, the model could be extended to multiple cavities by consequently adding the reflection term from each cavity [1]. This brings on added complexity and steady state solution becomes complex to obtain.

Approaches based on three mirror cavity is well explained by [5–8]. This model is based on principle that - by placing the (vibrating) external target in front of laser, an additional external cavity is formed. By periodically vibrating remote external target, the optical path difference (OPD) between the laser facet and the target changes, this in turn modifies the equivalent reflection of the laser facet and hence the OOP is also modulated. Again, this model is based solely on the reflection coefficients of the boundaries of the cavities, i.e., laser's facet (forming the laser cavity) and the target (forming additional external cavity).

#484086 https://doi.org/10.1364/OE.484086
Journal © 2023 Received 26 Dec 2022; revised 27 Mar 2023; accepted 30 Mar 2023; published 2 May 2023

Optics EXPRESS

SMI has been widely used for measurement from physical quantities - displacement [9], velocity [10,11], distance [11], vibration [12], imaging [13], acoustic detection and imaging [14] to name a few. Recently it has found its application in biophotonics such as pulse wave detection [15,16], and variety of other applications summarized well in [17].

Despite the exponential growth of SMI as non-contact, and non-destructive testing, theoretical background targeting biophotonics applications where the laser has to interact with multiple cavities filled with diffusive media having different reflection coefficient, attenuation coefficient and refractive index is not explained well. These parameters are particularly important for sensing biological samples e.g. system on chip, in vitro and/or in vivo biosensing, and also equally well desirable for industrial applications. So far in the current state of the art most of the models consider (a) single external cavity and (b) phase of the reflected field but not the attenuation of the electromagnetic field in individual cavities. The attenuation of the optical field in the external cavity, among many others, are important parameter as they determine the fringe visibility of the SMS and ultimately enable its detection. The dependence of the attenuation coefficient of the material forming the external cavity (cavities) and the reflection coefficient at the boundaries is important, in particular, in the case of diffusive materials which need to be characterized. So far, they have not been taken into account while explaining SMI phenomenon. Unlike, reflection from rigid body, where the reflection is considered to come from a point on the reflecting target, this does not hold true while considering diffusive media. In this case, reflection from multiple particles has to be taken into account. Multiple particles reflect electromagnetic radiation incident from laser differently due to its motion resulting in complex signal composing of many individual SMS due to each particle. In this regard, authors in [18,19], proposed a model to explain the multi scattering phenomenon from diffusive target, its implication on SMS and how to retrieve the individual velocity component of flowing particle in diffusive media. However, again the attenuation of the incident laser beam as it propagates through different media such as glass substrate, and channel is not taken into account. Taking attenuation into account in the model, this could benefit in tuning the laser emission power and/or different other parameters (described in detail in subsequent sections) to get optimal SMS resulting in improved velocity estimation of the particles. To overcome these limitations, we propose generalized multi-cavity SMI based on scattering theory.

Scattering matrix theory is widely used in describing the travelling wave in electrical networks with multiple impedance mismatch. The scattering matrix (S matrix) relates the amplitude of the reflected and incident waves at any interface, while transmission matrix (T matrix) relates the fields of one side of the interface to the other. Both matrices are equivalently used depending upon the desired analysis of the parameters under study. It has widely been used, e.g., in microwave circuits [20]. The same concept may be applied to explaining the optical wave propagation in the laser, and OF as well. It was first used by Wang et al. for analysis of interferometric and ring lasers [21]. Lau et. al. used it to describe a three junction triangular ring wave guide laser [22]. [23] analysed scattering loss in DFB lasers due to the presence of the grating. Coldren et al. used S and T matrix both to determine the equivalent reflection and transmission coefficients in groove coupled lasers, and two section coupled resonator systems [24,25].

In this paper, starting with basics of scattering theory in sec. 2, sec. 3 exploits scattering theory to determine modified equivalent reflection coefficient of coupled cavity in terms of both attenuation coefficient and phase constant (propagation constant) for single external cavity (SMI with single external cavity). Further, detail mathematical formalization is used to deduce standard equation of equivalent reflection coefficient [1,26] from the proposed model. The detailed joint effect of the reflection, attenuation coefficients, and their contribution to the resonance under optical feedback is then studied. Next, in sec. 4, utilizing the cascade properties of S and T matrix, the effect of OF from a single external cavity is extended to situations where multiple cavities are involved (multi cavity SMI). It is shown by just changing the boundary conditions

Optics EXPRESS

in a recursive way, the optimal condition for the effective coupling of the reflected optical field from multiple cavities in terms of *individual* cavity parameters such as cavity length, attenuation and reflection coefficients, or losses is presented. With the aid of mathematical background and simulation, it is demonstrated that the parameters of laser and the individual cavities can be tuned to obtain maximal SMS with higher fringe visibility. Further, in sec. 5, the concept is generalized, and algorithm is presented to obtain equivalent coefficient of the laser facet in presence of OF from N external cavity (generalized N cavity SMI). Finally, a conclusion in sec. 6 ends the chapter. The major contributions presented in this article are as follows:

1. We extend the scattering theory to SMI with one external cavity. We demonstrate that the equivalent reflection coefficient is a function of propagation constant i.e. attenuation coefficient and phase constant both (contrast to only phase constant as defined in compound cavity model [1,2,26]). Further we demonstrate mathematically that our proposed model based on scattering theory is a generalised laser equation in presence of SMI and reduces to standard lasing equation as described in [26] (Eq. 9.1) and [1] (appendix) when attenuation coefficient is equated to zero.

2. We demonstrate that the proposed scattering theory for OF can be extended to multiple cavities. The formalisation based on scattering theory is recursive and multiplicative such that the N external cavities can be expressed in terms of individual cavities $i = 1, 2 \cdots N-1$. Based on this, we define the equivalent reflection coefficient of laser cavity in presence of two external cavities (one laser cavity plus two external cavities), and then present a general equation of equivalent reflection coefficient of laser facet in presence of N external cavities which to our knowledge has not been demonstrated before. Further exploiting the general description, we demonstrate that how the scattering theory enables to tune individual cavities parameters to get optimal SMI with optimal fringe visibility.

2. Basics of scattering theory

In general, for a two port system like the one shown in Fig. 1(a), the reflected and incident field are related the to scattering coefficient, given by S and T matrices. S matrix, gives the transmission and reflection coefficient are determined in a single measurement. s_{11} and s_{21} (first column) give information about the reflection and transmission coefficient for a field incident from the left and s_{22} and s_{12} (second column) give information about the reflection and transmission coefficient for a field incident from the right. Similarly, T matrix relates the quantity on the left side (the forward wave) of the port to the quantity on the right side (the backward wave). Mathematically S and T matrices is given by [21,23–25]. The detailed derivation can also be found at [27]

$$\text{S matrix}: \quad \begin{bmatrix} b_1 \\ a_2 \end{bmatrix} = \begin{bmatrix} r & t' \\ t & -r \end{bmatrix} \begin{bmatrix} a_1 \\ b_2 \end{bmatrix}; \quad \text{T matrix}: \quad \begin{bmatrix} a_1 \\ b_1 \end{bmatrix} = \begin{bmatrix} \frac{1}{t} & \frac{r}{t} \\ \frac{r}{t} & \frac{1}{t} \end{bmatrix} \begin{bmatrix} a_2 \\ b_2 \end{bmatrix} \tag{1}$$

where r and t are the reflection and transmission coefficients at interface 1; and t' is the transmission coefficient at interface 2.

For the basic case of transmission in lossless medium without discontinuities (Fig. 2(a)), the S and T matrix are given by [21,23–25]

$$\text{S matrix}: \quad \begin{bmatrix} b_1 \\ a_2 \end{bmatrix} = \begin{bmatrix} 0 & e^{j\beta l} \\ e^{j\beta l} & 0 \end{bmatrix} \begin{bmatrix} a_1 \\ b_2 \end{bmatrix}; \quad \text{T matrix}: \quad \begin{bmatrix} a_1 \\ b_1 \end{bmatrix} = \begin{bmatrix} e^{-j\beta l} & 0 \\ 0 & e^{j\beta l} \end{bmatrix} \begin{bmatrix} a_2 \\ b_2 \end{bmatrix} \tag{2}$$

where β and l are respectively the phase constant and the cavity length. It should be noted that, since the media does not have discontinuities, the coefficients $s_{ij} \in S$ and $t_{ij} \in T$ related to reflection are set to zero in Eq. (1).

Optics EXPRESS

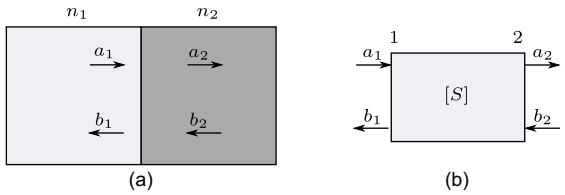

Fig. 1. Formalization of scattering matrix. (a) Wave propagation through medium of different refractive index. (b) Conversion to two port system.

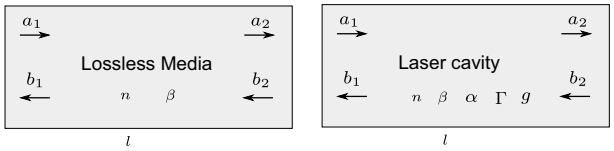

Fig. 2. Schematic diagram to obtain S and T matrix for different media. (a) Lossless and continuum media; (b) laser cavity with gain and attenuation.

Similarly, for the laser cavity (Fig. 2(b)) the associated loss (α), gain (g) and confinement factor (Γ) are introduced and the S and T matrix

$$\text{S matrix}: \quad \begin{bmatrix} b_1 \\ a_2 \end{bmatrix} = \begin{bmatrix} 0 & e^{j\beta l}e^{(\Gamma\frac{g}{2}-\frac{\alpha}{2})l} \\ e^{j\beta l}e^{(\Gamma\frac{g}{2}-\frac{\alpha}{2})l} & 0 \end{bmatrix} \begin{bmatrix} a_1 \\ b_2 \end{bmatrix} \tag{3}$$

$$\text{T matrix}: \quad \begin{bmatrix} a_1 \\ b_1 \end{bmatrix} = \begin{bmatrix} e^{-j\beta l}e^{-(\Gamma\frac{g}{2}-\frac{\alpha}{2})l} & 0 \\ 0 & e^{j\beta l}e^{(\Gamma\frac{g}{2}-\frac{\alpha}{2})l} \end{bmatrix} \begin{bmatrix} a_2 \\ b_2 \end{bmatrix} \tag{4}$$

3. Scattering theory applied to laser under optical feedback

In this section, the S/T matrix (relating the forward and backward field at an interface) is used to find the equivalent reflection coefficient of the laser facet in the presence of an external cavity formed by a target placed at distance L from laser. Further we relate the equivalent reflection coefficient to the optical output power (OOP) emitted from laser in presence of OF.

3.1. Equivalent reflection coefficient

Referring to Fig. 3, at interface 2, using S matrix,

$$\begin{bmatrix} b_3 \\ a_4 \end{bmatrix} = \begin{bmatrix} r_2 & t_2 \\ t_2 & -r_2 \end{bmatrix} \begin{bmatrix} a_3 \\ b_4 \end{bmatrix} \quad \Longrightarrow \; b_3 = r_2 a_3 + t_2 b_4 \quad | \quad a_4 = t_2 a_3 - r_2 b_4 \tag{5}$$

In the external cavity (between interface 2 and 3), using Eq. (3),

$$\begin{bmatrix} b_4 \\ a_5 \end{bmatrix} = \begin{bmatrix} 0 & e^{j\beta_1 L}e^{-\alpha_1 L} \\ e^{j\beta_1 L}e^{-\alpha_1 L} & 0 \end{bmatrix} \begin{bmatrix} a_4 \\ b_5 \end{bmatrix} \quad \Longrightarrow \; b_4 = e^{j\beta_1 L}e^{-\alpha_1 L} b_5 \quad | \quad a_5 = e^{j\beta_1 L}e^{-\alpha_1 L} a_4 \tag{6}$$

At interface 3, using Eq. (1), it reduces to

$$\begin{bmatrix} b_5 \\ a_6 \end{bmatrix} = \begin{bmatrix} r_3 & t_3 \\ t_3 & -r_3 \end{bmatrix} \begin{bmatrix} a_5 \\ b_6 \end{bmatrix}. \tag{7a}$$

Optics EXPRESS

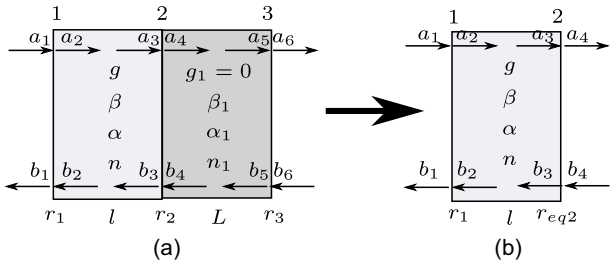

Fig. 3. Scattering theory applied to the analysis of OF. (a) Schematic diagram of the fields due to external target placed at a distance L from the laser. (b) Concept of equivalent cavity.

Using the new boundary conditions, $b_6 = 0$, as no beam enters the cavity system from behind the target

$$b_5 = r_3 a_5 \tag{7b}$$

$$a_6 = t_3 a_5 \tag{7c}$$

Putting the value of b_4 (from Eq. (6)) in Eq. (5), we get

$$b_3 = r_2 a_3 + t_2 b_5 e^{j\beta_1 L} e^{-\alpha_1 L} \tag{8}$$

using $b_5 b_4$ from Eq. (7b)

$$b_3 = r_2 a_3 + t_2 r_3 a_5 e^{j\beta_1 L} e^{-\alpha_1 L} \tag{9}$$

putting value of $a_5 b_4$ from Eq. (6) yields

$$b_3 = r_2 a_3 + t_2 r_3 a_4 e^{j2\beta_1 L} e^{-2\alpha_1 L} \tag{10}$$

using $a_4 b_4$ from Eq. (5), we get

$$b_3 = r_2 a_3 + t_2 r_3 (t_2 a_3 - r_2 b_4) e^{j2\beta_1 L} e^{-2\alpha_1 L} \tag{11}$$

$$b_3 = r_2 a_3 + t_2^2 r_3 a_3 e^{j2\beta_1 L} e^{-2\alpha_1 L} - t_2 r_3 r_2 b_4 e^{j2\beta_1 L} e^{-2\alpha_1 L} \tag{12}$$

placing the value of $t_2 b_4 b_4$ from Eq. (5) and $r_2^2 = 1 - t_2^2 b_4$ gets to the expression

$$b_3 = r_2 a_3 - r_3 r_2 b_3 e^{j2\beta_1 L} e^{-2\alpha_1 L} + r_3 a_3 e^{j2\beta_1 L} e^{-2\alpha_1 L} \tag{13}$$

$$b_3 (1 + r_2 r_3 e^{j2\beta_1 L} e^{-2\alpha_1 L}) = a_3 (r_2 + r_3 e^{j2\beta_1 L} e^{-2\alpha_1 L}) \tag{14}$$

$$r_{eq2} = \frac{b_3}{a_3} = \frac{r_2 + r_3 e^{j2\beta_1 L} e^{-2\alpha_1 L}}{1 + r_2 r_3 e^{j2\beta_1 L} e^{-2\alpha_1 L}} \tag{15}$$

$$= \frac{r_2 + r_3 e^{-2(\alpha_1 - j\beta_1) L}}{1 + r_2 r_3 e^{-2(\alpha_1 - j\beta_1) L}} \tag{16}$$

$$= \frac{r_2 + r_3 e^{-2\gamma_1 L}}{1 + r_2 r_3 e^{-2\gamma_1 L}} \tag{17}$$

where $\gamma_1 = \alpha_1 - j\beta_1$ is propagation constant of the field in the medium forming the external cavity and r_{eq2} is the equivalent reflectivity at interface 2 resulting from the external target placed at distance L (Fig. 3). Although the equation for equivalent reflection coefficient derived in Eq. (17) looks different in presence of attenuation coefficient and phase constant (propagation constant), this is the similar to standard equation obtained by different authors such as [26] (Eq. 9.1) and [1]. Putting the value of attenuation coefficient ($\alpha = 0$), Eq. (17) can be re-written in terms of

Optics EXPRESS

coupling coefficient, κ as proposed by [1,26]. The detail derivation of standard equations from Eq. (17) is derived in Appendix A.

In particular, referring to Fig. 3 and considering the general case where air is the medium in the external cavity formed by the second laser facet and the target, simulation are carried out to determine how the external parameters such as loss in external cavity ($\alpha_1 L$) and reflection coefficient of remoter target (r_3) affect the intrinsic properties of laser (equivalent reflection coefficient). From Fig. 4(a), it is observed that increasing the value of loss in external cavity ($\alpha_1 L$), the equivalent reflection coefficient of laser in presence of OF, r_{eq2} in general decreases. However, there exists a particular value of $\alpha_1 L$, (in this case it is 6×10^{-4}), for which a resonance is reached and r_{eq2} is minimal. Beyond this value, r_{eq2} increases again. It is also observed that for all the values of losses in the external cavity ($\alpha_1 L$), a minimal equivalent reflection coefficient is attained when the reflection coefficient of the external target is equal to that of the laser facet ($r_3 = r_2$).

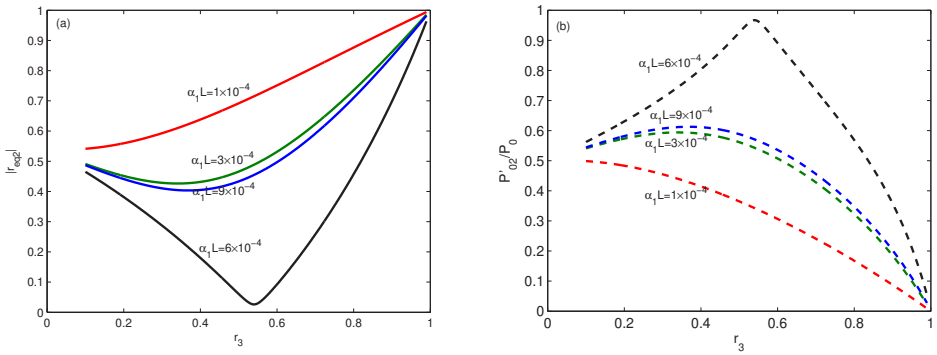

Fig. 4. Effect of the external cavity on the laser parameters. (a) Effect of loss in the external cavity ($\alpha_1 L$) on the equivalent reflectivity of laser under OF (r_{eq2}); (b) optical power emitted under OF normalized to total power of solitary laser (without OF). Simulation parameters $r_1 = r_2 = 0.54$, power output from solitary laser is unity (1 mW), power output from laser in presence of OF is obtained from Eq. (18), provided that r_{eq2} (defined in Eq. (17), is used (instead of r_2). In the absence of OF, $P_{02}/P_0 = 0.5$ (obtained by putting $r_1 = r_2$ in Eq. (18)). Simulation parameters - $\lambda = 692$ nm, $L = [0.2, \quad 0.06, \quad 0.12, \quad 0.18]$ m.

3.2. Optical output power

Another concerned parameter is the optical output power (OOP). Let P_0 be the total power emitted by the laser, P_{01} be the power out of the mirror having reflection coefficient r_1 (left surface in Fig. 3), and P_{02} power leaving the mirror with a reflectivity r_2 (the right surface, in Fig. 3). Obviously $P_0 = P_{01} + P_{02}$. The fraction of total power emitted from right surface is given by Eq. (18) [2,26–28].

$$\frac{P_{02}}{P_0} = \frac{(1 - r_2^2)}{(1 - r_2^2) + \frac{r_2}{r_1}(1 - r_1^2)} \tag{18}$$

Let us assume that the optical power output from laser is unity (1 mW). Although, laser has unequal reflection coefficient such that the emission is from one facet only. However for illustration purpose, we consider equal reflection coefficient here. Under this assumption, ($r_1 = r_2 = 0.54$), the power emitted from the laser P_{02} is halved i.e. 0.5 mW (obtained by putting $r_1 = r_2$ in Eq. (18). Simulation is carried under similar conditions to determine the effect of OF on and losses in the laser emission. Figure 4(b) shows the effect of OF on the power emitted by the laser, taking into account the losses in the external cavity ($\alpha_1 L$) at different values of external

Optics EXPRESS

reflection coefficient (r_3). In short, the power emitted under OF (P'_{02}) is obtained by replacing r_2 in Eq. (18), with the r_{eq2} value defined in Eq. (17). Unlike the results obtained in the case of r_{eq2}, increasing the losses in the external cavity ($\alpha_1 L$) brings on the increase in the power emitted by laser under OF (P'_{02}), which increases until a resonance is reached (in this particular case, at $\alpha_1 L = 6 \times 10^{-4}$). Beyond that value, the emitted power starts to degrade. It is also observed that in all of the cases, the maximal optical power emitted from the laser under feedback takes place when the external reflection coefficient equals the laser facet reflection coefficient i.e. when $r_3 = r_2$. Thus, by engineering the experimental conditions, the amount of losses in the external cavity and the reflection coefficient of the target, the conditions for laser emission under feedback can be optimized using the theory being proposed.

From Eqs. (16) and (17) backed by simulations, important conclusions are summarized below:

- Unlike [1,26] where the equivalent reflection coefficient (r_{eq2}) is dependent upon the reflection coefficient of the external target r_3, the phase constant β_1, the physical length L of the external cavity, and reflection coefficient of laser facet r_2, Eqs. (16) and (17) demonstrate that the equivalent reflection coefficient (r_{eq2}) is dependent upon attenuation coefficient α_1 as well thus the total loss incurred in the external cavity.

- Since the attenuation constant α_1 is a frequency dependent value, so will be the equivalent reflection coefficient, which will also vary with the frequency emission from the laser.

- For the total loss in external cavity and the reflection of the remote target, there exist a resonance condition where the equivalent reflection coefficient of laser facet is minimum and the optical output power (OOP) is maximal. Thus by tuning the loss (external cavity length), and the reflection coefficient of external target, the desired OOP emitted from can be achieved. Further since attenuation coefficient of medium is frequency dependent, the laser frequency emission can also be tuned to achieve desired OOP. The ability to tune the external parameters and/or parameter of laser to get desired OOP has profound implications in the use of bio-medical applications where the media is diffusive with different attenuation coefficient, reflection coefficient and refractive index.

Further, the strong dependence of r_{eq2} and P'_{02} on the external parameters (L, n_1) is the basis of self-mixing based. For instance, if the optical path between the laser and the external reflective target is modulated periodically by changing the physical length (L) (keeping the refractive index of the medium that forms the cavity constant) (Fig. 3), then the equivalent reflection coefficient r_{eq2} (Eq. (17)) is also modulated periodically introducing the well-know modulation of emitted power P'_{02}. Figure 5 further explains this effect. The physical length of the external cavity L is modulated ($L_{ext}(t) = L + L_{ext0} cos(2\pi ft)$) such that the peak modulation is $L_{ext0} = 3\lambda$, making the cavity length in the range $L_{ext}(t) \in L + L_{ext0}$. Such a modulation gets encoded in the optical power output of the laser, and is easily retrieved by processing such a power signal. In the absence of OF, as mentioned above, the power emitted from the laser is $P_{02} = 0.54$ mW and is a constant value (shown by dash line Fig. 5). However, in presence of OF and when the described modulation of optical path is introduced, it is no longer a constant and follows the modulation in OOP, being maxima or minima for each $\lambda/2$ change in phase gives rise to one fringes [10]. The appearance of six fringes for an induced displacement of 3λ (Fig. 5) is similar to that obtained from the standard equation of self-mixing for displacement measurement ($P_s = cos(4\pi L_{ext}(t)/\lambda)$) [10]. In addition to this information, the effect of r_3 in the SMS in terms of peak-to-peak value (pp) and fringe width is also presented. It is observed that at low $r_3 = 0.1$, the SMS is still weak and has a low pp value with wider fringes. At $r_3 = r_2 = 0.54$, a resonance is reached so the pp value of SMS increases drastically while the fringes are radically narrowed enabling easy and precise fringe detection through signal processing. This can also be interpreted as the laser has reached its maximal finesse. Finally, by detuning r_3=0.7, the SMS starts to degrade and widens again.

Optics EXPRESS

The observation of the resonance related to OF is coherent with Fig. 4(b), where a resonance in emitted optical power occurs when $r_3 = r_2$.

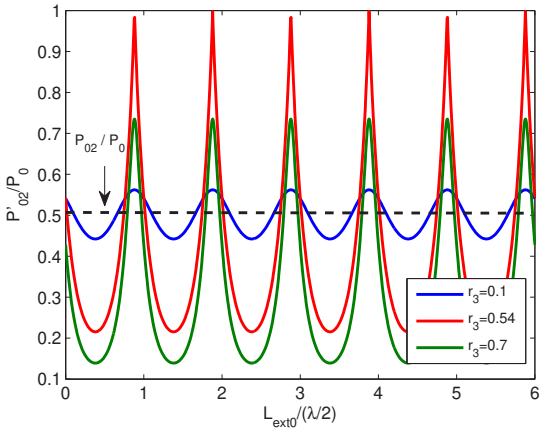

Fig. 5. Basic mechanism for the OF-based sensor. Modulation of OPL causes the modulation of emission power P'_{02}, which would have been constant without modulation of OPL (P_{02}). With the increase in r_3, the laser emission power increases and a resonance is reached when $r_3 = r_2$. Simulation parameters: $L_{ext0} = 3\lambda$; $r_1 = r_2 = 0.54$; n_1=1; $\lambda = 692$ nm; $\alpha_1 = 0.005/\text{m}$.

4. Laser with optical feedback from multiple cavities

So far, in the previous sections scattering was used to analyze the detailed response of the laser to OF from a single external cavity. The effect of reflection coefficient of the external target on the laser emission was shown in Fig. 5. Further, it was demonstrated that the resonance in laser emission is reached when the reflection coefficient of external target is close to that of laser facet. In this section, the same concept is extended to two external cavities with different cavity parameters, a situation relatively common when working with some transparent media, for instance in lab-on-chip applications, different area related to bio-photonics where diffusive media with different absorption and refractive index is encountered.

The different fields emanating from the two cavities are shown in Fig. 6(a). The setup is an extended version of the case of the external cavity just analyzed (Fig. 3). In the presence of a second external cavity (enclosed by interfaces 3 and 4), a set of additional new fields appear. The parameters that describe the second external cavity are designed as $g_2, \beta_2, \alpha_2, n_2$, where all the parameters have the same physical meaning of those listed in Table 1. Since, the S matrix for interface 1 to 3 is exactly the same presented in Eqs. (5), (6) and (7a) for the previous case analyzed, they are not repeated again.

Furthermore, in the second external cavity, defined by interfaces 3 and 4, the S matrix is given by

$$\begin{bmatrix} b_6 \\ a_7 \end{bmatrix} = \begin{bmatrix} 0 & e^{j\beta_2 L_2} e^{-\alpha_2 L_2} \\ e^{j\beta_2 L_2} e^{-\alpha_2 L_2} & 0 \end{bmatrix} \begin{bmatrix} a_6 \\ b_7 \end{bmatrix} \tag{19}$$

Finally, at interface 4

$$\begin{bmatrix} b_7 \\ a_8 \end{bmatrix} = \begin{bmatrix} r_4 & t_4 \\ t_4 & -r_4 \end{bmatrix} \begin{bmatrix} a_7 \\ b_8 \end{bmatrix} \tag{20}$$

Optics EXPRESS

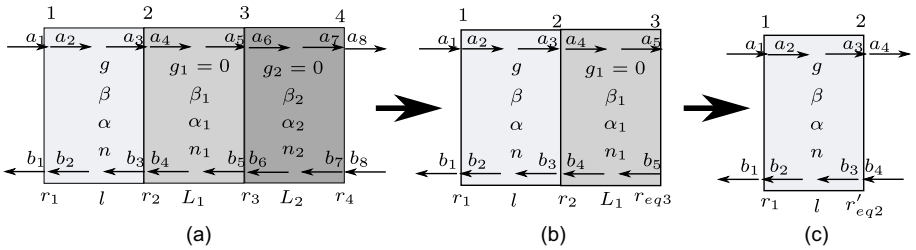

Fig. 6. Scattering theory for multi cavity optical feedback. $N = 2$ number of external cavity is simplified to single cavity in $N = 2$ recursive steps. (a) Field propagation in forward and backward direction under optical feedback from two external cavities. (b) Intermediate step converting two external cavity to one external cavity. (c) Converting the two cavities in (b) to a single cavity.

Table 1. List of relevant parameters involved in explaining laser dynamics in presence of OF.[a]

Description	Symbol
length of the laser cavity	l
length of external cavity	L
reflection coefficient at interface 1, 2, and 3	r_1, r_2, and r_3
confinement factor	Γ
laser gain per unit length	g
attenuation coefficient of material that form active region of laser	α
attenuation coefficient of material that form the external cavity	α_1
laser emission frequency	ω
phase constant of field in laser cavity	β
phase constant of field in the external cavity	β_1
refractive index of the material forming the first cavity	n_1
refractive index of the material forming the second cavity	n_2

[a]Interface 1 and 2 form the laser cavity and interfaces 2 and 3 form the external cavity in Fig. 3.

Using boundary condition, $b_8 = 0$

$$b_7 = r_4 a_7 \tag{21}$$

$$a_8 = t_4 a_7 \tag{22}$$

using the boundary condition $b_8 = 0$ (as no light enters the system from behind interface 4),and substituting b_7 from Eq. (21) in Eq. (19), enables to further solving Eqs. (19) and (7a) to get,

$$r_{eq3} = \frac{b_5}{a_5} = \frac{r_3 + r_4 e^{j2\beta_2 L_2} e^{-2\alpha_2 L_2}}{1 + r_3 r_4 e^{j2\beta_2 L} e^{-2\alpha_2 L_2}} \tag{23}$$

$$= \frac{r_3 + r_4 e^{-2\gamma_2 L_2}}{1 + r_3 r_4 e^{-2\gamma_2 L_2}} \tag{24}$$

where $\gamma_2 = \alpha_2 - j\beta_2$ is propagation constant of the medium forming the second external cavity, r_4 is the reflection coefficient at interface 4. (after loss $\alpha_2 L_2$ has occurred) of the material in the second cavity, and r_{req3} is the equivalent reflection coefficient at interface 3 resulting from the external target placed at distance L_1 (Fig. 6(b)). Now the problem of the two external cavities gets

Optics EXPRESS

reduced to the case of the single external cavity previously explained using Eq. (17), provided that r_3 in Eq. (17) is replaced by r_{eq3} (Eq. (24)). It is evident that the procedure proposed enables a setup with N external cavities which can be similarly converted into a single S matrix in N iterative steps. This observation is similar to the one in [23] when explaining scattering effects in DFB lasers.

Hence the overall equivalent reflection coefficient for the two external cavities is given by

$$r'_{eq2} = \frac{r_2 + r_{eq3}e^{-2\gamma_1 L_1}}{1 + r_2 r_{eq3}e^{-2\gamma_1 L_1}}. \tag{25}$$

The use of the scattering matrix has thus enabled to reduce the laser cavity and the two external cavities with different optical properties to a single characteristic equation for the laser operation, which when solved describes the response of the laser under the considered conditions.

4.1. Use case: Optimal design of multi cavity setup using scattering theory

One potential application of scattering theory could be to determine the optimal intermediate cavity length to get the maximal output power from the laser under OF in setups with multiple cavities. As an example, considering Fig. 6(a), assume the first external cavity (between interface 2 and 3) is filled with air, and the second external cavity (between interface 3 and 4) is filled with water or some solution under test (e.g., biological samples with media of different optical properties).Under these conditions, the optimal intermediate cavity length which attains the maximum optical power emitted from the laser is desirable, which corresponds to the minimal equivalent reflection coefficient. Simulations are carried out in MATLAB to see the effect of the external cavities on the performance of the laser, and presented in Fig. 7. Keeping the second cavity parameters constant at $\alpha_2 L_2 = 5 \times 10^{-3}$, n_2=1.33 and r_4=0.54, an optimal value of total losses $\alpha_1 L_1 = 5 \times 10^{-4}$ is obtained in the intermediate cavity for which the equivalent reflection coefficient is minimal (7(a)) and the power emitted from the laser is maximized 7(b). Detuning the loss from this value causes significant degradation in OOP.

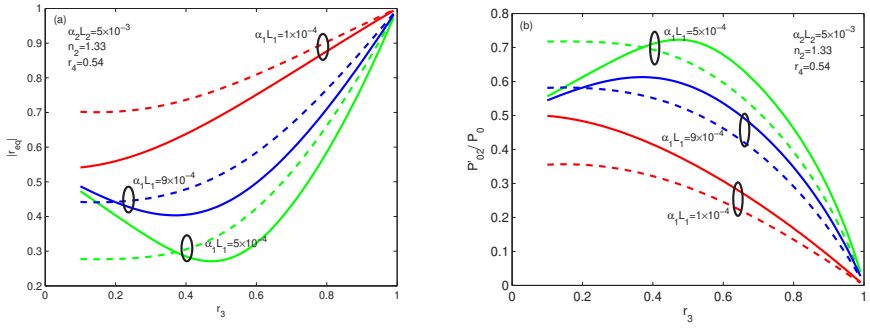

Fig. 7. Comparison between the (a) equivalent reflection coefficient calculated using scattering theory and (b) power emitted from laser P'_{02} in the cases of single (solid) and double (dashed) external cavities.

Further, two different conditions are studied: the response of the laser away from resonance ($r_3 \ll r_2$) and its response near resonance ($r_3 \cong r_2$). The former case is depicted in Fig. 8(a). The total loss in the intermediate cavity is kept fixed $\alpha_1 L_1 = 5 \times 10^{-4}$, and r_3 is set to 0.14, which in this case is the Fresnel reflection coefficient at the air ($n_1 = 1$) - water ($n_2 = 1.33$) interface). Then, the losses in the second external cavity $\alpha_2 L_2$ are varied in order to study its effects on the emitted power. Since for most of the cases, α_2 is a known value, basically varying loss is limited to varying the length of the second external cavity. It is observed that with an increase in r_4, the

Optics EXPRESS

power output from the laser under OF normalized to the power of the free-running laser decreases drastically and the rate of decrease increases with the decrease in the total losses in the second external cavity (which, known α_2, is understood as a reduction in length of the second external cavity). For the latter case, corresponding to the behaviour of the laser close to resonance, all the parameters are set as in the former case just described, provided that $r_2 \cong r_3 = 0.5$ (Fig. 8(b)). It is observed that the response of the laser can be divided in three regions. For the region $r_4 < r_3$, with an increase in r_4 the optical power output from laser increases, and its slope also increases with the decrease in total losses ($\alpha_2 L_2$) in the second external cavity. This means that, in this region, the shorter external cavity (with less losses) yields more power from the laser under feedback as compared to the free running laser at constant r_4 (unlike the previous case, where the optical power decreased with r_4). This is well illustrated by an example. Keeping $\alpha_2 L_2 = 0.025$ (red curve), increasing r_4 from 0.2 to 0.4, ratio of powr in SMS to solitary laser emission power increase from 0.6 to 0.7 as compared to 0.5 to 0.6 for the case when $\alpha_2 L_2 = 0.1$ (green curve). In the region $r_4 \cong r_3$ (more specifically $r_4 \cong r_3 \cong r_2$), the power output is maximal, although for different losses ($\alpha_2 L_2$) in the external cavity, resonance is reached at different r_4 values. This is an important conclusion as far as it states that the laser, under feedback from multiple cavities, presents a resonance condition dependent upon the losses in the second external cavity and its reflection coefficient. This result could be used to find the optimal second external cavity length for the most effective coupling of the light into the laser when under multiple cavity experiments, yielding an improved power output. This is particularly interesting in the case of highly diffusive samples under test where the power degrades with depth. Finally, the resonance for higher losses is obtained for $r_4 > r_3$, and the power drastically falls down. Since, the slope of the power curve decreases with the increase in losses in the second external cavity, so when at high r_4, it is desirable to work with larger cavity lengths, or higher loss, (at constant reflection coefficient) to optimize power output form the laser.

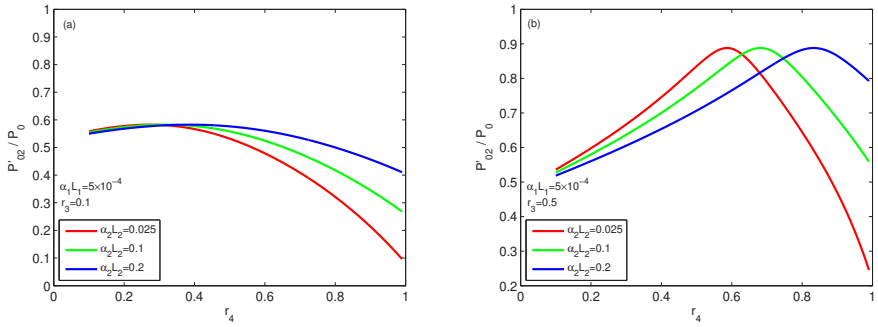

Fig. 8. Effect of second external cavity on power emission from laser according to scattering theory (a) away from resonance conditions (b) close to resonance conditions.

To complete the analysis of the double cavity case, it is desirable to study the fringe visibility of the SMS under different conditions. To do so, the parameters of both cavities are kept the same to those in Fig. 8 and the SMS corresponding to a target motion of 3λ is obtained. The amplitude of SMS is recorded for each target reflection coefficient r_4. Figure 9 shows the plot of amplitude of SMS as a function of r_4 at different external cavity loss conditions. For the case $\alpha_2 L_2 = 0.025$, when $r_4 = 0.1$, the SMS has a very low peak to peak value, resulting in fringes with reduced visibility and easily covered by noise in detection. Inset (b) in Fig. 9 shows the entire self-mixing waveform under this conditions. However, increasing r_4 to 0.6 (in close vicinity to resonance), makes the amplitude of the SMS to increase drastically. Inset (a) in Fig. 9 shows the complete waveform obtained in these conditions and it improvement when compared to inset (b). It is clear that tuning of the parameters associated with individual cavities (such as loss, cavity length

Optics EXPRESS

and reflection coefficient) can very significantly improve the SMS and fringe visibility can be maximized, and the SMS can be detected in presence of disturbances like speckle or different types of noise.

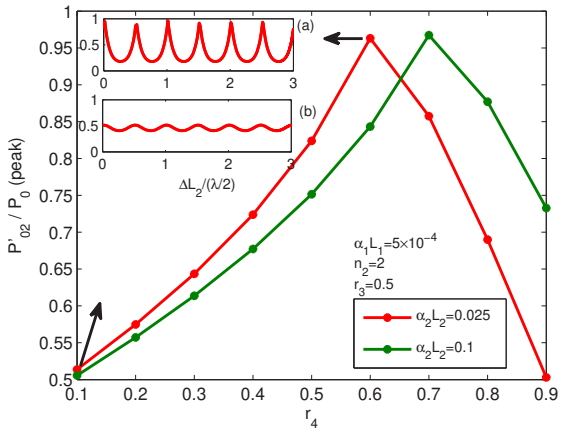

Fig. 9. SMS as a function of losses in external cavities and external reflection coefficient.

Thus conclusion drawn here is that

1. Each cavity parameters (loss, length and reflection coefficient) interact with one other in a way that there is a resonance condition for which the total loss in minimal and SMS power and fringe visibility is maximal. By tuning them, optimal experimental conditions can be achieved to get high fringe visibility of SMS.

2. With increase in loss in the cavity, the resonance shifts to higher value of reflection coefficient of the target to maintain the same SMS power and fringe visibility. This is better explained with an example - suppose we want the power to be 0.8. Then if the loss in external cavity is 0.025 (red), the reflection coefficient needs to be 0.48. Further, if the the loss in ext cavity is increased to 0.1 (green), the reflection coefficient needs to be 0.55.

5. Generalized scattering theory for N external cavities

Following sec. 3. (Eq. (17)), sec. 4. (Eq. (24)) and using mathematical induction, we can generalize the equivalent reflection coefficient of laser and OOP for N external cavities, given by Algorithm 1. Exploiting the matrix multiplication and recursive nature of scattering theory, we can extract the equivalent reflection coefficient and OOP at each individual interface as well.

6. Conclusion and discussion

The scattering theory, described using S and T matrices, is used as an effective tool to describe and characterize the effect of different external parameters in the performance of a solitary laser, of a laser with an external cavity under optical feedback, and of a laser with an external cavity with a vibrating target. The formalism enabled to include the effect of losses in every external media involved in the laser power output. It was shown that the expressions obtained can be used to describe the coupling of the optical field back into the laser cavity, and how the experimental setup provides some degrees of freedom which enable to optimize it in order to arrange an SMS with maximized visibility, given the parameters of the laser are known.

Beyond the very relevant result of quantifying the optimal arrangement for a single cavity self-mixing setup, a further strength of the method lies in the fact that N cascaded multiple

Optics EXPRESS

cavities can be explained extending the method in a recursive manner in N steps, calculating a final equivalent reflection coefficient. Further, such a multiple cavity model takes into account all the related external cavity parameters involved, including reflection coefficient, length, and losses all at once, including a explicit description of the effects of each individual cavity. In the case of OF with two cavities, the losses in each individual cavity were analyzed in detail, a case which usually is neglected elsewhere. It was quantified how losses or length in each external cavity affect the parameters of the other, and the overall response of the laser emission. Thus, a tuning is necessary between all the parameters to optimize the response, and scattering theory has proven to be an effective tool to model the overall response. However, analysis require accurate values of the external and internal cavity parameters to get reliable results, and the tuning gets more complex with the increase in the number of cavities. To address this, a simulation model of the experiment or digital twin can be leveraged to find the related relevant parameters and then use them in experiments in real world could be one among many other methods. This type of hybrid digital twin based approach has been already exploited by Zhao et al. in estimating the velocity of particles in diffusive media [18,19]. A further final conclusion is the behavioural complexity of single and multiple cavity systems under OF, which tremendously complicates the repeatability of the experimental conditions, a fact which is well known when working with self-mixing systems in the lab for accurate amplitude measurements.

Though, scattering theory proposed here explains the complexity of optical feedback and its effect in attaining a stable configuration when using multi-cavity self-mixing laser sensors, there are numbers of parameters in each cavity to be tuned to get optimal OOP. Because of recursive, cascaded and matrix operations involved, the model based on scattering theory could be extended to take the phase of reflection coefficient and laser emission polarization into account. Further, future work includes the experimental verification; developing a Deep neural network model to study the effect of laser and individual cavity parameters; and modify the proposed scattering theory to the diverse use case such as modelling multiple scatter from diffusive media [18,19].

Algorithm 1. Generalized scattering theory for N external cavities.

Input: Number of external cavities, N; attenuation coefficient for material forming each of cavity i, α_i; phase constant of the material forming the cavity i, β_i; propagation constant of material forming the cavity, $\gamma_i = \alpha_i + \beta_i$; length of external cavity i, L_i; laser cavity length, l; reflection coefficient of laser facets, r_1, r_2; reflection coefficient of the external cavity i, $r_{2:N+1}$; power emitted from solitary laser, P_{02}

Output: Equivalent coefficient, r_{eq2}; OOP, P'_{02}

for i=N to 2 **do**

  $r_{eqj} \leftarrow \frac{r_j + r_{j+1} e^{-2\gamma_{j-1} L_{j-1}}}{1 + r_j r_{j+1} e^{-2\gamma_{j-1} L_{j-1}}}$

  $r_j \leftarrow r_{eqj}$

end for

$P'_{02} \leftarrow \frac{1 - r_{eq2}^2}{(1 - r_{eq2}^2) + \frac{r_{eq2}}{r_1}(1 - r_1^2)} P_0$

return r_{eq2}, P'_{02}

A. Derivation of standard laser equation under OF from scattering theory

In this appendix, we demonstrate that the equivalent reflection coefficient as derived from scattering theory (Eq. (17)) is a general form. It can take different forms under different assumptions. For example, equating the attenuation coefficient in Eq. (17) to zero, the equivalent reflection coefficient as described in [1,26] can be attained.

Optics EXPRESS

Equating attenuation coefficient in Eq. (17) to zero and re-writing it as follows

$$r_{eq2} = \frac{r_2 + r_3 e^{2\beta_1 L} + r_2^2 r_3 e^{j2\beta_1 L} - r_2^2 r_3 e^{j2\beta_1 L}}{1 + r_2 r_3 e^{2\beta_1 L}} \tag{26}$$

It should be noted that the addition of the last two terms in the numerator of Eq. (26) cancels each other, so effectively it is the same as Eq. (17). Further, the first and third terms, and the second and fourth term are grouped, resulting in

$$r_{eq2} = \frac{r_2(1 + r_2 r_3 e^{j2\beta_1 L}) + r_3(1 - r_2^2) e^{j2\beta_1 L}}{1 + r_2 r_3 e^{j2\beta_1 L}} \tag{27}$$

$$= r_2 + \frac{r_3(1 - r_2^2) e^{j2\beta_1 L}}{1 + r_2 r_3 e^{j2\beta_1 L}} \tag{28}$$

using $\kappa = (1 - r_2^2) r_3 / r_2$ [26] and $t_2^2 = 1 - r_2^2$

$$r_{eq2} = r_2 + \frac{\kappa r_2 e^{j2\beta_1 L}}{1 + r_2 r_3 e^{j2\beta_1 L}} \tag{29}$$

Using Euler's formula $e^{j\theta} = cos(\theta) + jsin(\theta)$, and considering that the reflection coefficient is a real quantity (i.e., ignoring the imaginary part of Eq. (29)); $r_2 < 1$ and $r_3 < 1$, their product $r_2 r_3 << 1$; the maximum value of $cos(\theta)$ is 1, so the condition $r_2 r_3 cos(2\beta_1 l) << 1$ holds true, Eq. (29) reduces to

$$r_{eq2} = r_2 + \kappa r_2 cos(2\beta_1 L) \tag{30}$$

$$= r_2(1 + \kappa cos(2\beta_1 L)) \tag{31}$$

Equation (31) is exactly the same obtained in [1,26]. Thus it is evident that the Eq. (17) is the equivalent reflection coefficient that takes different forms as derived by different authors [1,26] under different conditions.

Disclosures. The authors declare no conflicts of interest.

Data availability. Data underlying the results presented in this paper are not publicly available at this time but may be obtained from the authors upon reasonable request.

References

1. R. Lang and K. Kobayashi, "External optical feedback effects on semiconductor injection laser properties," IEEE J. Quantum Electron. **16**(3), 347–355 (1980).
2. K. Petermann, "External optical feedback phenomena in semiconductor lasers," IEEE J. Sel. Topics Quantum Electron. **1**(2), 480–489 (1995).
3. S. Donati, "Laser interferometry by induced modulation of the cavity field," J. Appl. Phys. **49**(2), 495–497 (1978).
4. G. Acket, D. Lenstra, A. Den Boef, and B. Verbeek, "The influence of feedback intensity on longitudinal mode properties and optical noise in index-guided semiconductor lasers," IEEE J. Quantum Electron. **20**(10), 1163–1169 (1984).
5. K. Petermann, *Laser Diode Modulation and Noise* (Kluwer Academic Publishers, 1991).
6. T. Bosch, N. Servagent, and S. Donati, "Optical feedback interferometry for sensing application," Opt. Eng **40**(1), 20–27 (2001).
7. R. Kliese, T. Taimre, A. A. A. Bakar, Y. L. Lim, K. Bertling, M. Nikolić, J. Perchoux, T. Bosch, and A. D. Rakić, "Solving self-mixing equations for arbitrary feedback levels: a concise algorithm," Appl. Opt. **53**(17), 3723–3736 (2014).
8. P. Chen, Y. Liu, B. Gao, and C. Jiang, "Modeling and experimental verification of laser self-mixing interference phenomenon with the structure of two-external-cavity feedback," Opt. Commun. **410**, 690–693 (2018).
9. D. Guo, L. Shi, Y. Yu, W. Xia, and M. Wang, "Micro-displacement reconstruction using a laser self-mixing grating interferometer with multiple-diffraction," Opt. Express **25**(25), 31394–31406 (2017).
10. A. Jha, F. J. Azcona, C. Y. nez, and S. Royo, "Extraction of vibration parameters from optical feedback interferometry signals using wavelets," Appl. Opt. **54**(34), 10106–10113 (2015).

Optics EXPRESS

11. M. Norgia, D. Melchionni, and A. Pesatori, "Self-mixing instrument for simultaneous distance and speed measurement," Opt. Lasers Eng. **99**, 31–38 (2017).
12. A. Jha, F. J. Azcona, and S. Royo, "Frequency-modulated optical feedback interferometry for nanometric scale vibrometry," IEEE Photonics Technol. Lett. **28**(11), 1217–1220 (2016).
13. H. S. Lui, T. Taimre, K. Bertling, Y. L. Lim, P. Dean, S. P. Khanna, M. Lachab, A. Valavanis, D. Indjin, E. H. Linfield, A. G. Davies, and A. D. Rakić, "Terahertz inverse synthetic aperture radar imaging using self-mixing interferometry with a quantum cascade laser," Opt. Lett. **39**(9), 2629–2632 (2014).
14. K. Bertling, J. Perchoux, T. Taimre, R. Malkin, D. Robert, A. D. Rakić, and T. Bosch, "Imaging of acoustic fields using optical feedback interferometry," Opt. Express **22**(24), 30346–30356 (2014).
15. A. Arasanz, F. Azcona, S. Royo, A. Jha, and J. Pladellorens, "A new method for the acquisition of arterial pulse wave using self-mixing interferometry," Optics & Laser Technology **63**, 98–104 (2014).
16. F. F. M. de Mul, J. van Spijker, D. van der Plas, J. Greve, J. G. Aarnoudse, and T. M. Smits, "Mini laser-doppler (blood) flow monitor with diode laser source and detection integrated in the probe," Appl. Opt. **23**(17), 2970–2973 (1984).
17. J. Perchoux, A. Quotb, R. Atashkhooei, F. J. Azcona, E. E. Ramirez-Miquet, O. Bernal, A. Jha, A. Luna-Arriaga, C. Yanez, J. Caum, T. Bosch, and S. Royo, "Current developments on optical feedback interferometry as an all-optical sensor for biomedical applications," Sensors **16**(5), 694 (2016).
18. Y. Zhao, J. Perchoux, L. Campagnolo, T. Camps, R. Atashkhooei, and V. Bardinal, "Optical feedback interferometry for microscale-flow sensing study: numerical simulation and experimental validation," Opt. Express **24**(21), 23849–23862 (2016).
19. L. Campagnolo, "Optical feedback interferometry sensing technique for flow measurements in microchannels," Doctoral Thesis, Institut National Polytechnique de Toulouse (INP Toulouse) (2013).
20. K. Kurokawa, "Power waves and the scattering matrix," IEEE Trans. Microwave Theory Tech. **13**(2), 194–202 (1965).
21. S. Wang, H. K. Choi, and I. H. A. Fattah, "Studies of semiconductor lasers of the interferometric and ring types," IEEE J. Quantum Electron. **18**(4), 610–617 (1982).
22. S. T. Lau, T. Shiraishi, and J. M. Ballantyne, "Scattering matrix analysis of a triangular ring laser," J. Lightwave Technol. **12**(2), 202–207 (1994).
23. Q. Y. Lu, W. H. Guo, R. Phelan, D. Byrne, J. F. Donegan, P. Lambkin, and B. Corbett, "Analysis of slot characteristics in slotted single-mode semiconductor lasers using the 2-d scattering matrix method," IEEE Photonics Technol. Lett. **18**(24), 2605–2607 (2006).
24. L. Coldren, K. Furuya, B. Miller, and J. Rentschler, "Etched mirror and groove-coupled GaInAsP/InP laser devices for integrated optics," IEEE J. Quantum Electron. **18**(10), 1679–1688 (1982).
25. L. A. Coldren, K. J. Ebeling, B. I. Miller, and J. A. Rentschler, "Single longitudinal mode operation of two-section GaInAsP/Inp lasers under pulsed excitation," IEEE J. Quantum Electron. **19**(6), 1057–1062 (1983).
26. K. Petermann, *Laser Diode Modulation and Noise* (Kluwer Academic Publishers, 1988).
27. A. Jha, "Continuous wave frequency modulated optical feedback (CWFM-OF): Theory and Applications," Doctoral Thesis, Departament of Optics and Optimetry, Technical University of Catalunya (2016).
28. C. Lin, C. Burrus, and L. Coldren, "Characteristics of single-longitudinalmode selection in short-coupled-cavity (scc) injection lasers," J. Lightwave Technol. **2**(4), 544–549 (1984).